International Journal of Mass Spectrometry 462 (2021) 116532

Contents lists available at ScienceDirect

International Journal of Mass Spectrometry

journal homepage: www.elsevier.com/locate/ijms

Quantitative assessment of six different reagent gases for charge transfer dissociation (CTD) of biological ions

Zachary J. Sasiene [a], Praneeth M. Mendis [a], Glen P. Jackson [a, b, *]

[a] C. Eugene Bennett Department of Chemistry, West Virginia University, Morgantown, WV, 26506-6121, USA
[b] Department of Forensic and Investigative Science, West Virginia University, Morgantown, WV, 26506-6121, USA

ARTICLE INFO

Article history:
Received 4 December 2020
Received in revised form
20 January 2021
Accepted 21 January 2021
Available online 27 January 2021

Keywords:
Radical ions
Kinetic energy
Ion activation
Ion fragmentation
Ion beam
Tandem mass spectrometry

ABSTRACT

Charge transfer dissociation mass spectrometry (CTD-MS) has been shown to induce high energy fragmentation of biological ions in the gas phase and provide fragmentation spectra similar to extreme ultraviolet photodissociation (XUVPD). To date, CTD has typically employed helium cations with kinetic energies between 4-10 keV to initiate radical-directed fragmentation of analytes. However, as a reagent, helium has recently been listed as a critical mineral that is becoming scarcer and more expensive, so this study explored the potential for using cheaper and more readily available reagent gases. A model peptide, bradykinin, and a model oligosaccharide, κ-carrageenan with a degree of polymerization of 4, were fragmented using a variety of CTD reagent gases, which included helium, hydrogen, oxygen, nitrogen, argon and lab air. The CTD results were also contrasted with low-energy collision-induced dissociation (LE-CID), which were collected on the same 3D ion trap. Using constant reagent ion fluxes and kinetic energies, all five alterative reagent gases generated remarkably consistent sequence coverage and fragmentation efficiencies relative to He-CTD, which suggests that the ionization energy of the reagent gas has a negligible effect on the activation of the biological ions. The CTD efficiencies of all the gases ranged from 11-13% for bradykinin and 7-8% for κ-carrageenan. Within these tight ranges, the abundance of the CTnoD peak of bradykinin and the efficiency of CTD fragmentation of bradykinin both correlated with the ionization energy of the CTD reagent gas, which suggests that resonant charge transfer plays a small role in the activation of this peptide. The majority of the excitation energy for bradykinin and for κ-carrageenan comes from an electron stopping mechanism, which is described by long-range interactions between the reagent cations and electrons in the highest occupied molecular orbitals (HOMOs) of the biological ions. The CTD spectra do not provide any evidence for covalently bound products between the biological ions and the more-reactive gases like hydrogen, oxygen and nitrogen, which implies that the high kinetic energies of the reagent ions make them unavailable for covalent reactions. This work demonstrates that any of the substitute reagent gases tested are viable options for future CTD-MS experiments.

1. Introduction

Mass spectrometry is an important tool in the field of biomolecule analysis and has recently achieved a major milestone of detecting 10,000 proteins in only 100 minutes on a single instrument [1]. High resolution accurate mass (HRAM) measurements, such as those made by orbitrap instruments, have helped improve the confidence in identifying the product ions in tandem mass spectra [2–4]: however, HRAM measurements of intact molecular ions only provides the elemental formula and not the constitutional arrangement of the atoms. Tandem mass spectrometry (MS/MS), and most commonly collision-induced dissociation (CID), helps provide the structural information about selected precursors [5]. Most hybrid instruments rely on the use of 2D or 3D quadrupole ion traps (QITs) to achieve collisional activation of selected precursors [6–8] combined with faster scanning or higher-resolution mass spectrometers like time-of-flight and Orbitrap mass analyzers, respectively, to acquire the resultant product ion spectra [9–11].

In the analysis of biomolecules such as peptides, CID often cleaves the most labile bonds, which, in addition to generating

* Corresponding author. Prof. Glen P Jackson West Virginia University C. Eugene Bennett Department of Chemistry, Morgantown, WV, 26506-6121, United States.
E-mail address: glen.jackson@mail.wvu.edu (G.P. Jackson).

https://doi.org/10.1016/j.ijms.2021.116532
1387-3806/

important amide cleavages, also produces peaks corresponding to uninformative internal fragments and one or more neutral losses [12–14]. Another problem in the development of CID in QITs is the limited mass range of the product ion spectra, which originates from the requirements to effectively trap high mass precursor ions while co-storing low mass product ions [15–17]. In practice, the low mass cut off (LMCO) value is typically set to approximately 1/3 of the mass of the precursor ion, so product ions below this threshold are generally not observable in product ion spectra. Attempts to overcome the LMCO limitations of ion traps have included the use of pulsed DC potentials [18,19], performing CID during mass acquisition [20–23] and applying short durations of high amplitude RF excitation before subsequently lowering the trapping RF amplitude [24,25]. Others have overcome the limitations of CID by developing entirely new methods of ion activation, including fragmentation using electrons [26,27], metastable atoms [28–31], ions [32–36] photons [37–40] and surfaces [41–43].

Charge transfer dissociation mass spectrometry (CTD-MS) [44,45] is a radical-driven fragmentation technique that evolved from cation-cation reactions conducted by the groups of Zubarev [32] and Schlathölter [33,34]. CTD performs similarly to extreme ultraviolet photodissociation (XUVPD) [46,47], but is applicable on bench-top mass spectrometers and on precursors in all charge states except -1 [44–47]. The modifications required to conduct CTD-MS are similar to those described for MAD-MS [28] and have been described in detail elsewhere [44,45]. In short, CTD uses a saddle-field fast ion source placed above a pre-drilled 3D ion trap to enable pulses of kiloelectronvolt reagent gas cations to enter the ion trap and activate the isolated precursors. Kinetic energies in the range of 3-10 keV help overcome the cation-cation coulombic barrier and provide practical fragmentation efficiencies above 5%. During CTD, precursor ions are not kinetically excited, so, unlike CID, precursor ions can be held at q_z values that enable product ions to be collected that are significantly below the typical CID limit of 1/3 the mass of the precursor. One major downside to CTD is that the LMCO does influence the background signal of CTD spectra, and the chemical background seems to be dependent on side reactions of the CTD beam with residual gases and vacuum pump oil [48].

To date, CTD-MS has demonstrated some appealing capabilities in common with other high energy activation techniques, including: 1) the production of cross-ring cleavages and the preservation of labile modifications, such as sulfate groups in the analysis of oligosaccharides [46,49,50]; 2) the cleavage of disulfide linkages in the analysis of proteins [51]; 3) the generation of side chain losses in the analysis of peptides, which can be helpful in the differentiation of isomeric peptides [48]; 4) the localization of double bond positions in phospholipids [52]; and 5) the differentiation of β-1,4- and β-1,3-linkage isomers in native oligosaccharides [53].

One drawback of CTD-MS is the reliance on ultra-high-purity helium as a reagent gas, especially given the ongoing helium shortage crisis [54–57]. Helium was recently placed on the US critical minerals list, and US congress has met to discuss alternative options to technologies that require helium [58,59]. High-priority uses of helium include magnetic resonance imaging (MRI) in hospitals, nuclear magnetic resonance (NMR) instruments in chemistry facilities and major particle accelerators etc., and it would be helpful if non-essential helium-dependent techniques could be performed without the use of helium. In metastable atom activated dissociation mass spectrometry (MAD-MS), the differences in the internal energies and ionization energies of the metastable atoms of different noble gases had a measurable impact on the product ion spectra [28,29,31,60]. For example, MAD-MS of peptides and lipids using He metastable atoms consistently produced intact oxidized product ions in addition to fragment ions; however, Ar metastable atoms typically did not produce intact oxidized product ions. In contrast to MAD, the present study shows that the nature of the reagent gas ions appears to have very little effect on the abundance and types of product ions formed in CTD. These quantitative results are based on replicate measurements of a model peptide, bradykinin, and of a sulfated oligosaccharide, κ-carrageenan, which has a degree of polymerization of four (dp4). Both analytes, but bradykinin in particular, have been extensively characterized using a variety of activation techniques [29,47–49,60–63].

2. Experimental

2.1. Sample preparation

Bradykinin was purchased from Sigma-Aldrich (St. Louis, MO, USA) and was used without further purification. The bradykinin standard was prepared into a working solution of 100 ppm in acetonitrile and water (1:1) with 1% acetic acid. The acetonitrile was Optima LC/MS grade whereas the acetic acid was ACS reagent grade, and both were purchased from Fisher Scientific (Fair Lawn, NJ, USA). The water was obtained from a Milli-Q purification system (Burlington, MA, USA).

The κ-carrageenan dp4 oligosaccharide was produced at the CNRS-UPMC UMR 8227 research unit of the Station Biologique de Roscoff, France. κ-Carrageenans from Euchema Cottonii (CPKelco) were degraded into oligosaccharides using the enzyme κ-carrageenase and were then purified with preparative size exclusion chromatography [49]. A working solution of κ-carrageenan dp4 was then prepared at 100 ppm in water/heptylamine/methanol (25/25/50). HPLC grade methanol was purchased from Fisher Scientific (Fair Lawn, NJ, USA) and the ion pair reagent (IPR) heptylamine was purchased from Alfa Aesar (Ward Hill, MA, USA).

2.2. Instrumentation

All experiments were conducted on a modified Bruker amaZon 3D Ion Trap (Bruker Daltonics, Bremen, Germany) [44] that was custom modified with a saddle-field fast ion source (VSW/Atomtech, Macclesfield, UK) placed directly above a 2 mm hole in the ring electrode of a 3D ion trap. A variable leak valve controlled the amount of gas supplied to the CTD ion source, which typically raised the pressure of the main vacuum chamber to ~$1x10^{-5}$ mbar (uncorrected). The ion source was connected to an Ultravolt HVA series high voltage power supply (Advanced Energy, Denver, CO, USA) that was pulsed from ground to high voltage with rise times as fast as 5 ns using a Behlke 101-03 switch (Behlke, Billerica, MA, USA). The ion source was triggered by the TTL signal from the MS^2 event of the Bruker amaZon and sent to an Agilent 33250A arbitrary function generator (AFG) (Keysight Technologies, Santa Rosa, CA, USA), which provided a delay and pulse width that was independently variable of the MS^2 event in the software. A DS1054 digital oscilloscope (Rigol, Beaverton, OR, USA) compared the trigger waveform from the AFG with the scan function of the Bruker amaZon to ensure that the high voltage pulses coincided with the desired storage period of the scan function.

2.3. Method

All experiments were conducted in positive polarity mode with the instrument operated in manual MS/MS mode. Bradykinin was analyzed using the standard Apollo electrospray ionization (ESI) source (Bruker, Billerica, MA, USA) with a flow rate of 5 μL/min, a capillary voltage of -3500 V and a dry gas temperature of 220 °C. Precursor ions were isolated with an isolation window of 4 Da and

then activated by the reagent cation beam for a duration of 100 ms at a kinetic energy of 5.1 keV and a flux of 5 μA. Different reagent gases required slightly different flow rates to achieve the constant flux and energy conditions. The LMCO was set to *m/z* 250 to aid in the removal of ionized pump oil fragments, and product ions were stored for 250 ms after the 100 ms reaction to reduce the abundance of background ions with *m/z* values below 300. The isolated precursor abundance for bradykinin was kept constant at approximately $3x10^6$ counts to permit the quantitative comparison of fragmentation efficiencies between the different reagent gases. CTD fragmentation efficiencies were calculated based on the sum of the product ion signal relative to the abundance of precursor ion signal before CTD activation.

Due to the limited sample volume, κ-carrageenan dp4 was analyzed using static nanospray ionization (NSI) with Econo 12-N-pulled borosilicate emitters (New Objective, Woburn, MA, USA). The capillary voltage was -1500 V and the dry gas temperature was 100 °C. The parameters used for the isolation and activation of κ-carrageenan dp4 were the same as for bradykinin, except that the kinetic energy and flux of the reagent cation beam were kept constant at approximately 4.25 keV and 0.5 μA, respectively, for the different reagent gases.

The different reagent gases were lab air, ultra-high purity (UHP) argon, UHP helium, UHP hydrogen, UHP oxygen and UHP nitrogen, with the UHP gases purchased from Matheson Tri-Gas (Fairmont, WV, USA). The UHP gases had a purity of 99.999%, except oxygen, which had a purity of 99.98%. For the experiments with lab air, the gas line was simply disconnected, and the leak valve sampled the laboratory air at ~1 atm. To prevent contamination between the different gases, separate gas lines were employed for each gas, and the lines were both purged with the reagent gas and evacuated for >10 mins into the vacuum chamber at $<1x10^{-5}$ mbar before back-filling with the desired reagent gas. To reduce the negative effects of space charge on the product ion spectra, unreacted precursor ions were resonantly ejected between CTD activation and mass acquisition using 3 V for bradykinin and 1.5 V for κ-carrageenan dp4.

Bruker Compass Data Analysis 4.0 SP4 software was used for the data analysis. Microsoft Excel version 14 (Microsoft, Redmond, WA, USA) and ChemDraw 16.0 (PerkinElmer, Waltham, MA, USA) were used for mass spectral plots and chemical structures, respectively.

3. Results and discussion

3.1. Bradykinin

Before comparing the different reagent gases for CTD, CTD was first contrasted with traditional low-energy CID (LE-CID) on the same instrument. As an example, Fig. 1 shows a comparison of the MS^2 analysis of bradykinin with LE-CID and H_2-CTD. The LE-CID spectrum in Fig. 1a contains many neutral losses, a few b and y ions and two z ions, which is typical for CID of bradykinin [13]. In contrast, the H_2-CTD spectrum in Fig. 1b is considerably richer and has a variety of product ions—such as a, b, c, x, and y product ions—that provide comprehensive amino acid sequence information. As seen in Fig. 1b, H_2-CTD achieved nearly full sequence coverage whereas LE-CID achieved only 56% sequence coverage. The neutral losses observed in both product ion spectra correlate well with previous reports in which most of the neutral losses were identified as side chain losses [48,64–66].

Until the present study, CTD in our group has been performed exclusively using helium cations because the high ionization energy of helium (24.6 eV) was thought to be necessary to maximize the excess energy available to drive radical fragmentation of the precursor ions through a resonance charge transfer (electron capture) mechanism. However, in related work, the Schlathölter group has investigated electronic stopping and electron capture as two possible mechanisms to explain the observations of fast cation-cation reactions [33,34]. Electronic stopping refers to reactions in which the projectile ion induces electronic excitation of the target ion through long-range ion-electron interactions, whereas electron capture involves the resonant capture of electrons by the projectile from the highest occupied molecular orbital (HOMO) of the target ion.

Schlathölter's group found that for small peptides like bradykinin and for reagent cations in the region of 3-10 keV—which overlaps with the energies in the present work—the observed product ions were mostly immonium ions or side chain losses and were best explained by the electron capture mechanism. However, they note that the amount of energy deposited during the electron stopping mechanism increases—and therefore is likely to be more dominant—for targets that enable longer pathways through regions of higher electron density. Schlathölter's group also showed that the nature of the reagent gas had a very modest influence on the product ion spectra, with He^{2+} and H^+ tending to form some extra fragments above *m/z* 200 relative to He^+. However, in contrast to the present work, and for reasons that are not clearly evident, Schlathölter's group noted only a few fragments of low abundance above *m/z* 200 for various small peptides. Also, in the present work, the low mass cutoff of *m/z* 250 reduces the contribution of chemical background ions but prevents us from observing product ions below *m/z* 250. We therefore can't easily compare the full-range product ion spectra of our work with results from the Schlathölter group.

In other work involving high energy collisions between $[bradykinin+2H]^{2+}$ and He neutrals, Nielsen et al. found that acceleration voltages up to 50 kV provided an abundance of a ions [67,68]. They attributed the formation of these a ions to charge-remote fragmentation [67,68]. As described previously, helium cations at ~5 keV produce a distribution of fragment types from the 2+ precursor of bradykinin, but a stronger contribution of a and x ions from the 1+ precursor (Fig. 1b) [51]. In agreement with Nielsen et al., we note that, in addition to abundant a and x ions from the 1+ precursor of bradykinin, CTD tends to form y_7" and y_8" ions in preference to the y_7 and y_8 ions observed in low energy CID (Fig. 1a).

Although cleavage on the N-terminal side of proline residues is generally favored in the formation of both the y- and y"-type ions, low-energy CID provides time for mobile protons to drive charge-directed cleavages and form the y_7 and y_8 fragments. In contrast, the higher activation energies in CTD and keV-CID tend to favor the charge-remote fragments, y_7" and y_8". In related work, Poulter et al. performed CID of $[bradykinin+H]^+$ [69] at collision energies of ~6 keV and also found an abundance of a ions and a preference for y_7" and y_8" ions over y_7 and y_8 ions. These comparisons demonstrate the consistency of H_2-CTD with other studies involving the interaction of gas-phase peptides with neutrals and ions in the range of 1-10 keV in the laboratory frame.

Fig. 2 shows a comparison between He-CTD and O_2-CTD of the 1+ precursor of bradykinin. Upon cursory inspection, the spectra appear almost identical, with only minimal differences apparent on closer inspection. Both spectra show neutral losses from the precursor that are characteristic of radical-directed side chain losses. As described previously [48], the neutral losses of 43, 44, 59, 60, 87, 99 and 100 Da are all characteristic of side chain losses from arginine residues [64,66,70,71], and the loss of 91 Da is characteristic of a side chain loss from phenylalanine [65]. Many of these side chain losses were also observed as product ions by the Schlathölter group [33,34].

One subtle difference between the He-CTD and O_2-CTD spectra is that the improved signal-to-noise ratio of the He-CTD spectrum

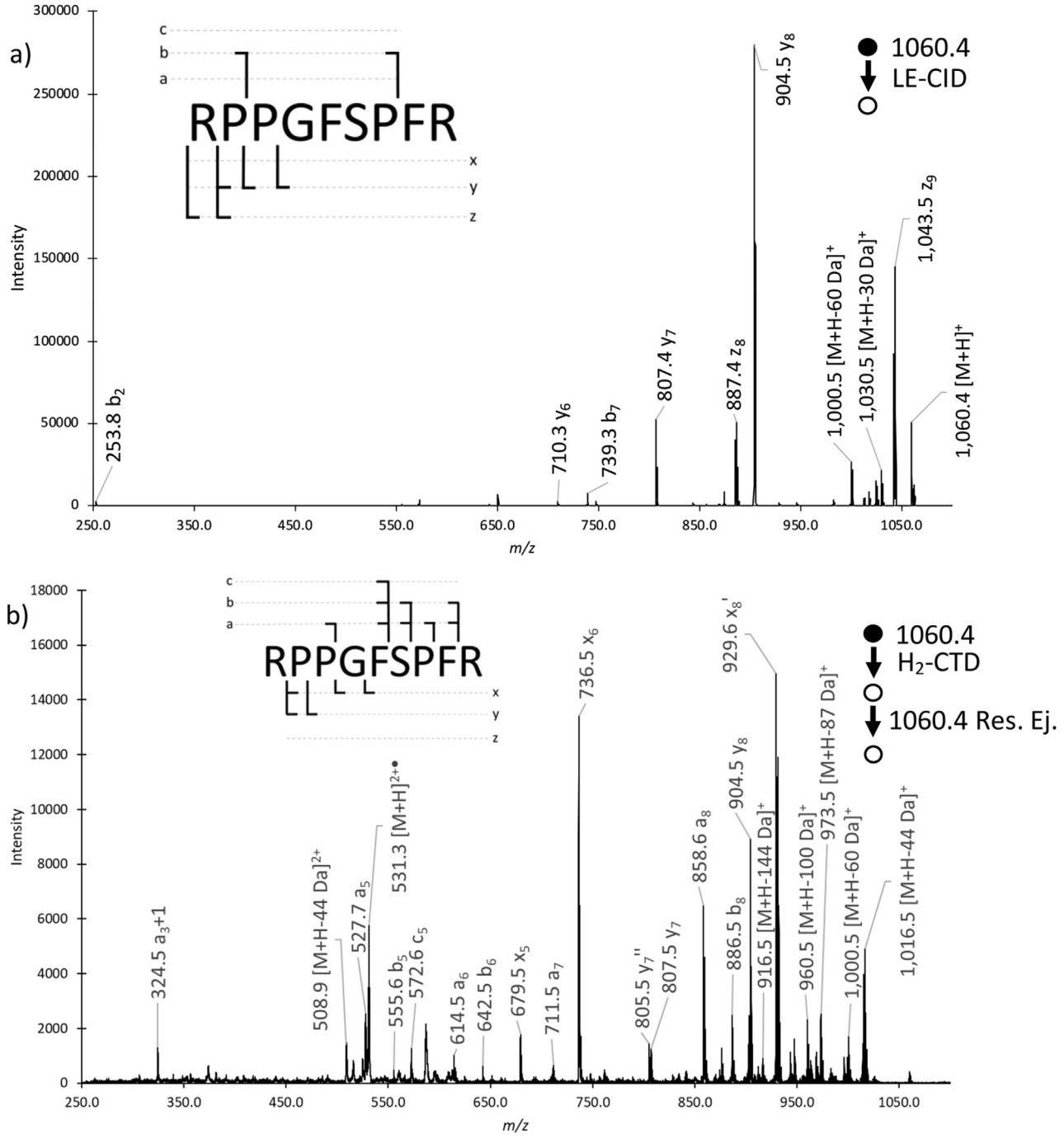

Fig. 1. Product ion mass spectra of bradykinin with insets of the product ion map for each activation technique: a) LE-CID of $[M+H]^+$ precursor at *m/z* 1060.4 with an excitation amplitude of 0.9 arbitrary units; b) H_2-CTD of $[M+H]^+$ precursor at *m/z* 1060.4 with resonance ejection of unreacted precursor ions at *m/z* 1060.4 before mass acquisition.

enables the observation of a few additional product ions, including the a_7, b_5, b_6, x_4, and z_6' product ions. However, only the a_7 product ion provides new sequence coverage relative to the other shared fragments. The increased abundance of the peaks in He-CTD could be due to the differences in ionization energy between helium cations at 24.6 eV and oxygen cations at 12.1 eV, which enables He cations to provide more energy for fragmentation via the charge-transfer mechanism. Another difference in the He-CTD and O_2-CTD spectra is the abundance of the CTnoD peak, $[M+H]^{2+\bullet}$, at *m/z* 531.3. This product ion is the simple charge transfer product ion, and He-CTD provides a ~3x more abundant CTnoD peak compared to O_2-CTD. Again, the increased efficiency in the He-CTD spectrum is presumed to be related to the ~12-eV difference in ionization energy between the O_2^+ and He^+ cations.

Tandem mass spectra for the lab air-CTD, N_2-CTD and Ar-CTD of bradykinin can be found in Figures S1 and S2. The spectra share major similarities in the overall pattern of peaks that are formed. However, there are subtle differences in the overall signal-to-noise ratios, which influences the ability to identify some of the less abundant product ions. Table S1 displays the average signal-to-noise ratio for *m/z* 531.3 and *m/z* 736.4 present in all the CTD spectra of bradykinin. The abundance of the CTnoD peak is also

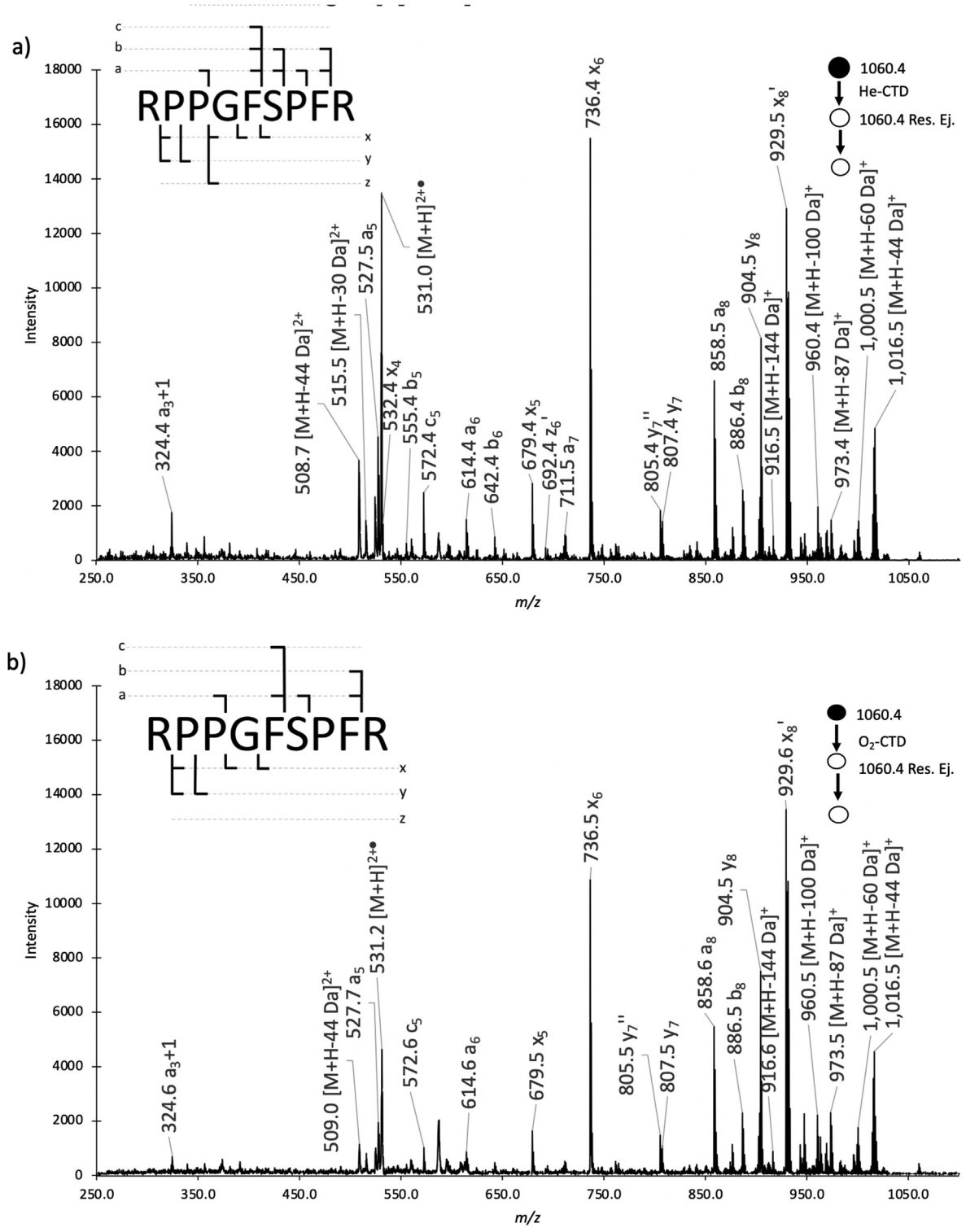

Fig. 2. Product ion mass spectra of bradykinin with insets of the product ion map for each activation technique: a) He-CTD of $[M+H]^+$ precursor at *m/z* 1060.4 with resonance ejection of unreacted precursor ions at *m/z* 1060.4 before mass acquisition; b) O_2-CTD of $[M+H]^+$ under identical conditions.

notably different between the different reagent gases. The use of chemically reactive gases like H_2, O_2 and N_2 did not introduce any observable covalent adducts, which indicates that chemical reactions between the fast reagent cations and the pseudo-stationary analyte cations are exclusively electronic in nature, in agreement with the theoretical considerations of the Schlathölter group [33,34].

Fig. 3 shows the product ion maps for Ar-CTD, lab air-CTD, H_2-CTD, O_2-CTD, He-CTD and N_2-CTD. The product ion maps for each reagent gas are remarkably similar, with near uniform sequence coverage for each gas and only slight differences in less-abundant product ions. The lab air-CTD and N_2-CTD have identical product

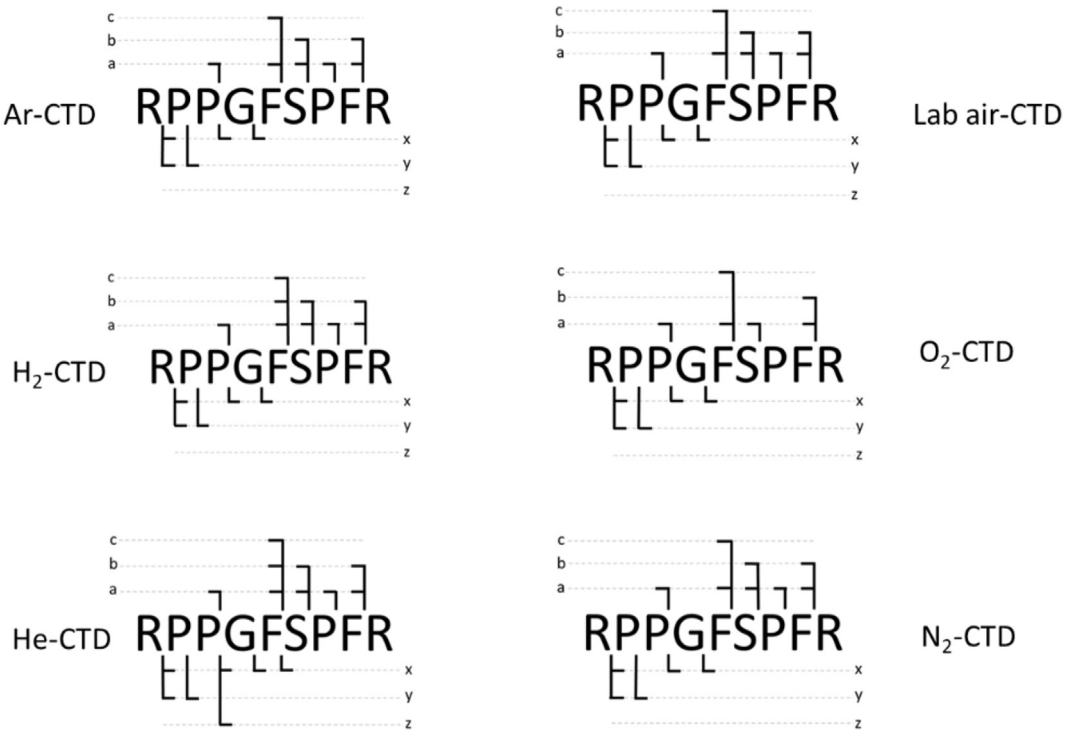

Fig. 3. Product ion maps for CTD of bradykinin using different reagent gases at the same kinetic energy of 4.25 keV.

ion maps, with only minor differences in the ion abundances, which is understandable given that lab air contains ~78% N_2. The similar electron affinities of nitrogen, argon, hydrogen and oxygen at 15.6 eV, 15.8 eV, 15.4 eV and 12.1 eV, respectively, could explain the general consistency in the product ions generated with these different reagent gases. However, given that the He-CTD is so similar to the other gases, yet has a considerably larger ionization energy than the other gases at 24.6 eV, indicates that the majority of the activation energy must derive from the kinetic energy of the ions. The corollary is that the ionization energy has a very modest effect on the distribution of product ions.

To allow for quantitative comparisons of the fragmentation efficiencies between the different reagent gases, the precursor ion abundance and the kinetic energy and flux of the reagent cations were all kept constant for each reagent gas. The CTD efficiencies of each gas are plotted as a function of ionization energy of the neutral gases in Fig. 4a. Note that reagent gas ions were not mass-selected from the ion gun, so we cannot exclude the possible contribution of atomic ions in the ion beams of the molecular reagent gases. The error bars show the 95% confidence interval based on five replicates of each reagent gas. Between each replicate, the reagent gas supply and power supply to the ion gun were turned off before re-establishing the desired conditions.

The fragmentation efficiencies for each reagent gas were remarkably consistent, between 11.5%-13.1%. Helium had the highest fragmentation efficiency of 13.1%. Approximately 75% of the variance in the abundance of the fragmentation efficiency can be explained by the variance in the ionization energy of the reagent gas, and the correlation was significant at the 99% confidence interval.

Pairwise t-tests were performed between each of the gases, and helium was statistically different from all the other gases, except argon, at the 95% confidence level. Ar-CTD was not significantly different than He-CTD because it provided such a large variance in replicate CTD efficiencies. The larger ionization energy of helium results in a higher fragmentation efficiency for bradykinin compared to the other reagent gases. Even though there were other statistical differences between the efficiencies of the different reagent gases (e.g. between H_2 and O_2), there was little practical significance between the fragmentation efficiencies because the efficiencies only differed, at the most, by 1.6%.

Fig. 4b is a scatter plot of the abundance of the CTnoD peak for bradykinin verses the ionization energy of the reagent gas. The ionization energies provided are for the neutral atoms and molecules in the legend of Fig. 4. As mentioned above, the reagent ion beam was not mass filtered, so the exact identity and purity of the reagent ion beam cannot be conclusively assigned for each reagent gas. According to the linear regression line in Fig. 4b, approximately 75% of the variance in the abundance of the CTnoD peak can be explained by the variance in the ionization energy of the reagent gas, and although the slopes are shallow, the correlation was significant at the 99% confidence interval. As might be apparent in Fig. 4a and b, the abundance of the CTnoD peak also showed a significant correlation with the fragmentation efficiency, with a coefficient of correlation (R^2) of 0.73 (plot not shown). These results indicate that the abundance of the CTnoD oxidation product, $[M+H]^{2+\bullet}$, correlates strongly with the CTD efficiency and is therefore a likely intermediate in the fragmentation pathway to other product ions.

Helium has the highest ionization energy of the reagent gases studied, and because it provides the highest efficiencies—albeit by a half a percent—the electron capture mechanism must play a small, but statistically significant, role in the ionization and fragmentation of the peptide. Despite this finding, the trivial differences in 1) sequence coverage, 2) background contaminant levels, 3) CTnoD product ion abundance, and 4) fragmentation efficiencies of the different reagent gases implies that any of the alternative reagent gases—including lab air and nitrogen—can be considered as possible alternatives for the analysis of small peptides like bradykinin. This finding is not necessarily a recommendation,

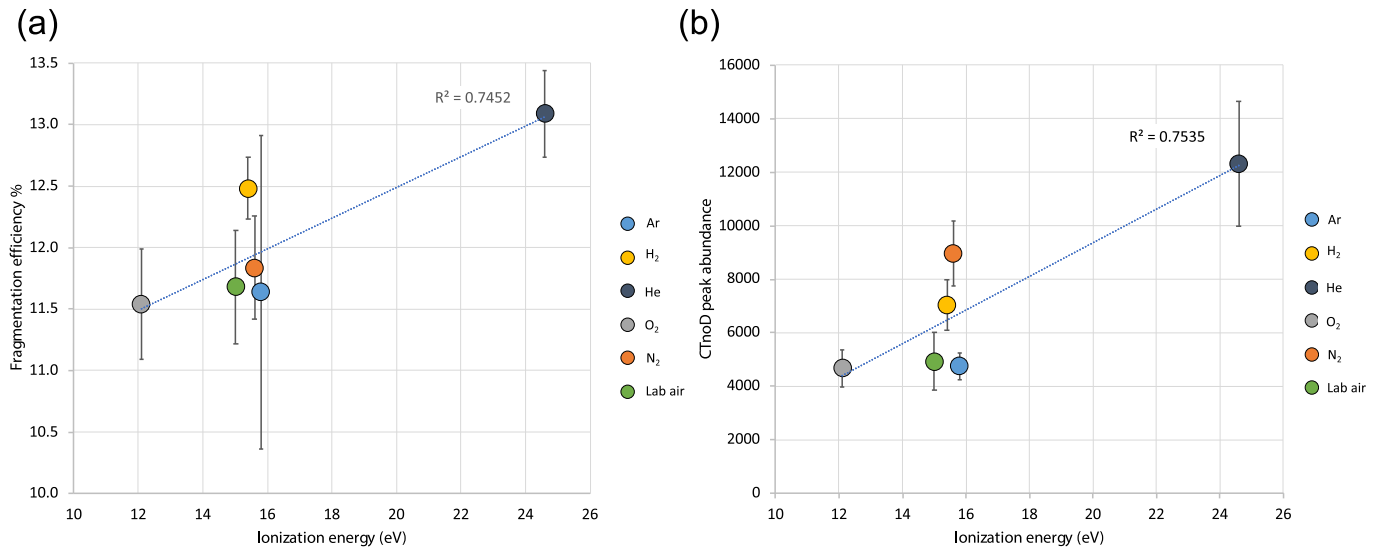

Fig. 4. CTD fragmentation efficiencies and CTnoD peak abundances for the fragmentation of bradykinin using different CTD reagent gases. Error bars show the 95% confidence interval for N=5 replicate experiments.

however, because certain electrical components, like the electron multiplier, may be sensitive to moisture and oxygen in the different reagent gases.

3.2. κ-Carrageenan dp4

The κ-carrageenan oligosaccharide selected for this work has a degree of polymerization of four (dp4) and is composed of alternating anhydro-D-galactose and sulfated D-galactose monomers with *O*-sulfation present at the 2nd and 4th monomer. Fig. 5 shows a comparison of LE-CID and He-CTD of the $[M+IPRH]^+$ precursor at *m/z* 1136.4, where IPRH is the protonated ion pair reagent heptylamine. The IPR was added to simulate the types of ions formed during ion-pair reagent-reversed phase-HPLC (IPR-RP-HPLC) [47].

The LE-CID spectrum of κ-carrageenan dp4 (Fig. 5a) generated a few glycosidic cleavages and many neutral losses from the precursor, including $[M+IPRH-H_2O]^+$, $[M+IPRH-SO_3]^+$ and $[M+IPRH-IPR]^+$ (i.e. $[M+H]^+$). The LE-CID spectrum contained no cross-ring cleavages, and the information acquired from the LE-CID spectrum was therefore insufficient to localize the sulfate groups or even determine which monomer contained the sulfate groups. In contrast to the LE-CID spectrum, the He-CTD spectrum displays extensive fragmentation, including glycosidic and cross-ring cleavages, which localized the sulfate groups to the second and fourth sugars. The Z_3 and B_2 product ions were able to localize one sulfate to the D-galactose unit on the nonreducing end, and the Z_1 product ion localized another sulfate group to the D-galactose unit closest to the reducing end. The $^{0,2}A_4$ and the $^{1,4}A_4$ product ions narrowed the location of the sulfate group to either the C3 or C4 position on the sulfated D-galactose monomer on the reducing end, and given that carrageenans typically only have sulfate groups on the C2, C4 or C6 positions [72,73], the second sulfate group can confidently be assigned to the C4 position.

For the sulfated D-galactose on the second Gal unit, the $^{2,5}A_2$ product ion in the various CTD spectra of Figs. 5b and 6 indicates that the sulfate is located at the C3, C4, C5 or C6 position. Due to the aforementioned sulfate patterns in κ-carrageenans, the sulfate position can be restricted to the C4 or C6 position but cannot be definitively assigned to either position within the second residue.

Fig. 6a shows a product ion spectrum of κ-carrageenan dp4 that was fragmented using lab air-CTD. The spectrum is almost indistinguishable from the He-CTD spectrum in Fig. 5b. The same glycosidic and cross-ring fragments that are present in the He-CTD spectrum are also present in the lab air-CTD spectrum and both provide the same level of specificity for locating the sulfate positions. For the He-CTD and lab air-CTD spectra, the anhydro-D-galactose monomers only have $^{0,2}X_n$, $^{1,5}X_n$, $^{0,2}A_n$ and $^{1,5}A_n$ cross-ring cleavages because the anhydro bridge prevents the observation of cleavage products within the 3,6 anhydro bridge. The anhydro bridge would require two covalent bond cleavages within the ring to enable the fragments to separate with measurable results. The types of ions and abundances of ions for He-CTD and lab air-CTD are also practically consistent with the Ar-CTD, N_2-CTD, O_2-CTD and H_2-CTD product ion spectra of κ-carrageenan dp4 in Fig. 6b–e. For example, the spectral similarities between spectra collected with the different CTD reagent gases relative to He-CTD were quantified using Pearson product-moment correlations (PPMCs). The PPMC values provided in Table S2 range from 0.9832 for lab air-CTD to 0.9924 for N_2-CTD.

Similar to the bradykinin results in Fig. 4, the efficiencies for the CTD fragmentation of κ-carrageenan dp4 in Fig. 7 show generally consistent CTD efficiencies among the different reagent gases. The fragmentation efficiencies range from approximately 7%-8%, with lab air-CTD providing the highest fragmentation efficiency of 8.1%, which is significantly different than the other gases (t-test, $P < 0.05$). Unlike the bradykinin results in Fig. 4, the variance in the fragmentation efficiency is not explained by the variance in ionization energy of the reagent gases, and the CTnoD peak is always absent in the κ-carrageenan spectra. One possible explanation for the differences in behavior between bradykinin and κ-carrageenan results could be that the ionization energy for bradykinin (i.e. $[M+H]^+ \rightarrow [M+H]^{2+\bullet} + e^-$) is larger than κ-carrageenan dp4. The larger ionization energy of bradykinin would cause more energy to be expended in the formation of the CTnoD peak, with less energy available for fragmentation. The general reduction in excess energy would provide a greater dependence on the recombination energy available from the reagent gases because some reagent ions would be able to overcome certain activation thresholds and others would not.

An alternative explanation for the differences in efficiency trends between the peptide and the oligosaccharide could be that there are stronger noncovalent forces in the higher order gas-phase

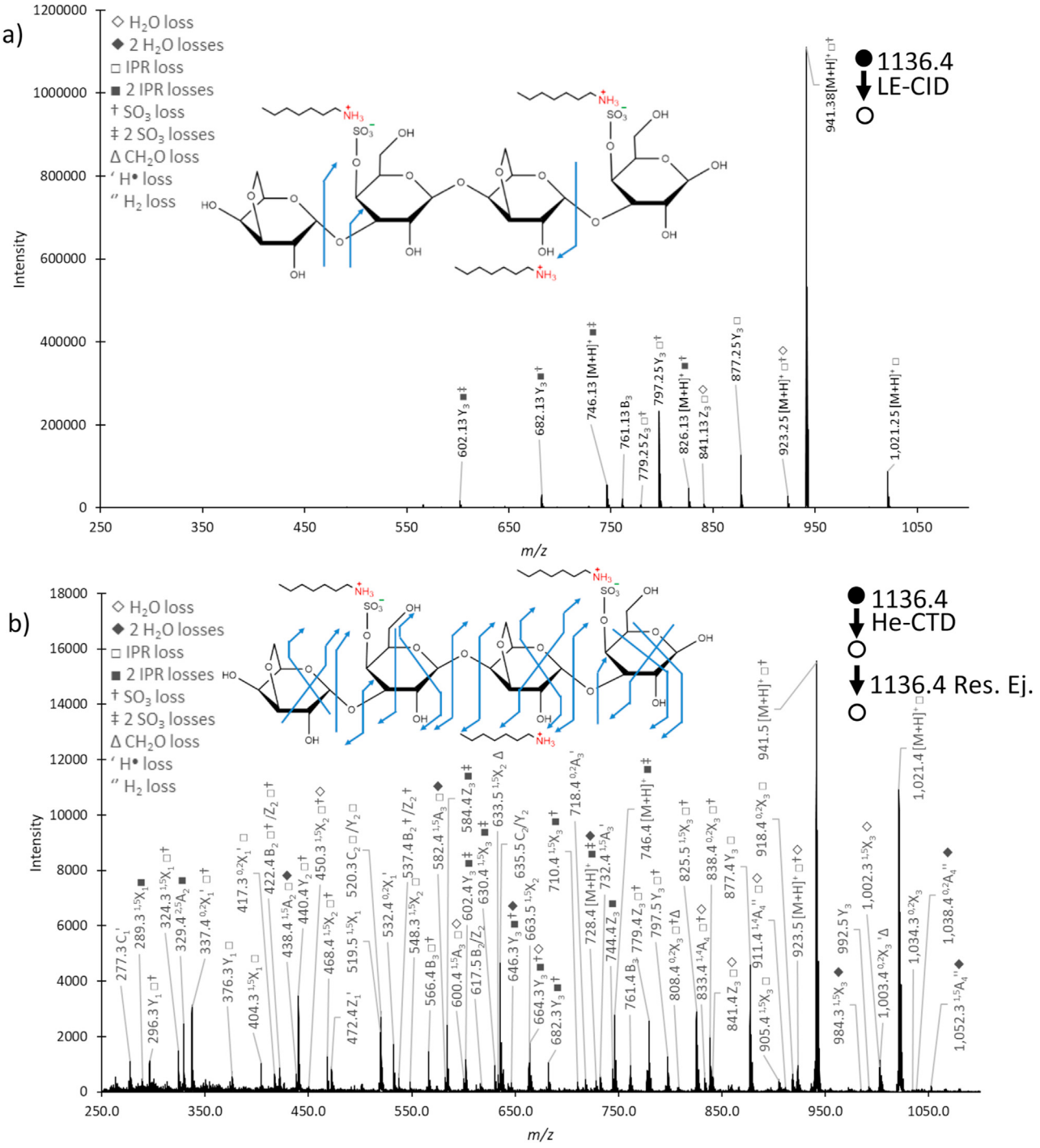

Fig. 5. Product ion mass spectra of κ-carrageenan dp4 with insets of the product ion map for each activation technique: a) LE-CID of $[M+IPRH]^+$ precursor at *m/z* 1136.4 with an excitation amplitude of 0.7 arbitrary units; b) He-CTD of $[M+IPRH]^+$ precursor at *m/z* 1136.4 with resonance ejection of unreacted precursor ions at *m/z* 1136.4 before mass acquisition.

structure of bradykinin, such as salt bridges between the arginine residues and the internal carbonyl groups [74], which form a more compact structure and enable the peptide fragments to stay together after the covalent bonds of the backbone are cleaved. However, the most likely explanation is provided by the Schlathölter group in their description of the electron stopping mechanism [33,34].

Schlathölter's group describe that when charged projectiles with kinetic energies in the kiloelectronvolt range pass through regions of high electron density in a target, the activation energy associated with electronic stopping can exceed 100 eV. The structure of κ-carrageenan dp4 has more electron-dense regions than bradykinin because of the numerous OH and sulfate groups. The excess energy afforded by the electron-rich sulfate groups of κ-carrageenan dp4 readily surpasses the energy required to form the CTnoD ion, and this excess energy increases the probability of fragmentation. Because all the reagent ions can activate the biological ions through the electron stopping mechanism, and because

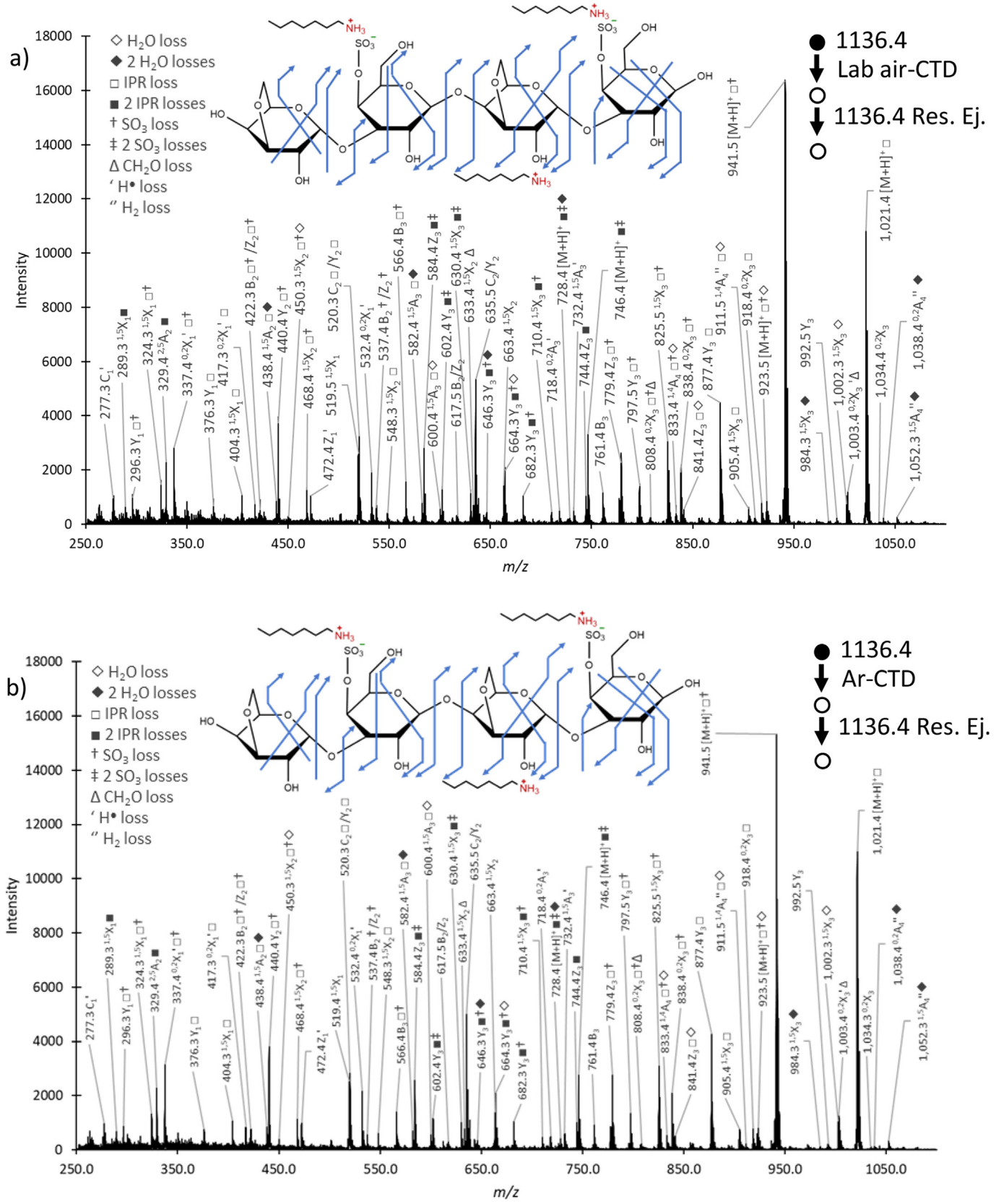

Fig. 6. Product ion mass spectra of κ-carrageenan dp4 with insets of the product ion map for each activation technique: a) Lab air-CTD of $[M+IPRH]^+$ precursor at *m/z* 1136.4 with resonance ejection of unreacted precursor ions at *m/z* 1136.4 before mass acquisition; b) Ar-CTD of $[M+IPRH]^+$ under identical conditions; c) N_2-CTD of $[M+IPRH]^+$ under identical conditions; d) O_2-CTD of $[M+IPRH]^+$ under identical conditions; e) H_2-CTD of $[M+IPRH]^+$ under identical conditions.

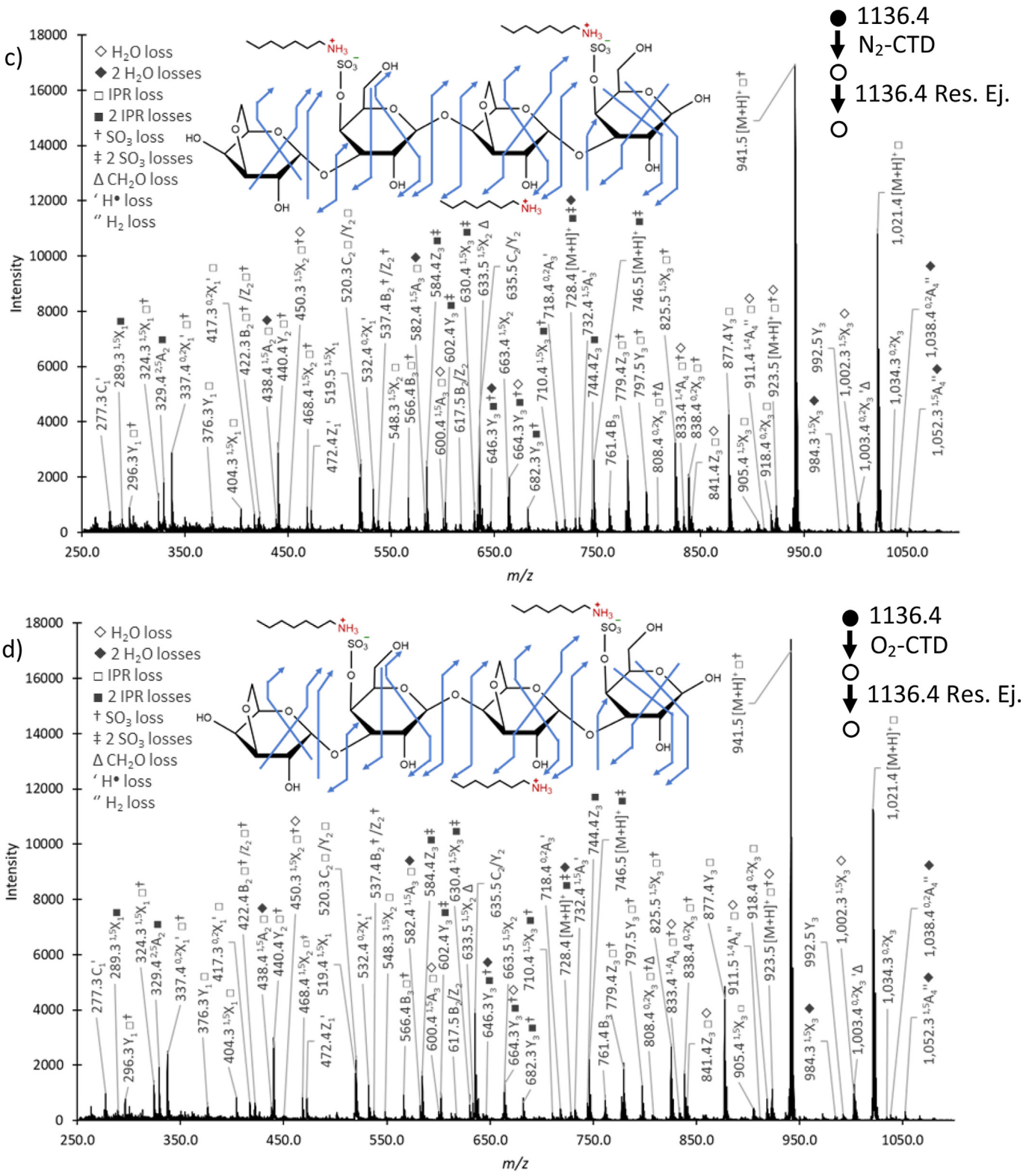

Fig. 6. (*continued*).

this pathway is more dominant than the charge transfer pathway for κ-carrageenan, the fragmentation efficiency of κ-carrageenan is less dependent on the ionization energy of the reagent gas, hence the horizontal trend line in Fig. 7.

Previously collected He-CTD data indicates that oligosaccharides that lack high electron dense regions are more inclined to provide a CTnoD peak [46], both because the ionization potential of the target ion becomes higher—so there is less excess energy for fragmentation—and because the charge transfer mechanism becomes more prominent as the electron density decreases. As described above, non-covalent internal bonds—like salt bridges and hydrogen bonds—may also cause some structures to stay intact as a CTnoD product after the backbone is cleaved.

Pairwise t-tests were also performed to determine any significant differences in the fragmentation efficiencies of the different reagent gases for κ-carrageenan. Although lab air-CTD was significantly different than all of the other reagent gases at the 95% confidence interval, the efficiencies are not meaningfully different because the efficiencies are all within 1% of one another. The general lack of significant difference in the CTD efficiencies of κ-carrageenan with the different reagent gases implies that the energy of activation is dominated less by the charge transfer mechanism and more by the kinetic energy of the reagent cations and the timescale of interaction. The apparent dominance of the electron stopping mechanism for κ-carrageenan therefore limits the contribution of resonant energy transfer between the reagent cations and electronic energy levels of the reactants [33,34].

As mentioned before, the propensity for the electron stopping mechanism is expected to be enhanced for target ions that are larger and/or with regions of high electron density, which presumably explains the two-electron oxidation process observed for the small protein, insulin [50]. Double oxidation was not observed here for κ-carrageenan. Based on the observations in the present work, we predict that the nature of the reagent gas would have little effect on the efficiency of the double oxidation mechanism of insulin because the mechanism of energy transfer should be dominated by the electron stopping mechanism, which deposits significantly more energy to the target ions than the charge transfer mechanism.

Previous studies involving He-CTD of carrageenans and porphyrans in negative ion mode have shown fragmentation efficiencies as high as 12% for iota-carrageenan dp4 in the 4- charge state [48], which is consistent with the theory that electron dense targets can gain more activation energy. However, it is unwise to infer too much about the mechanism of energy deposition by comparing the fragmentation efficiencies of different sugars with the same reagent gas because the location of the sulfate groups on the sugars can help direct specific back-bone cleavages [48] and therefore influence the fragmentation efficiencies.

Regarding the prospects for future studies and the importance of different reagent gas conditions, evidence from the Schlathölter group suggests that changes in the kinetic energy of the reagent ion beam within the range of 5-10 keV will have a negligible effect on both the energy deposited during activation and the distribution of products ions, but the velocity of the reagent ion beam scales linearly with energy deposited during activation [33,34], so the efficiency is expected to increase modestly with kinetic energy. The efficiency is also expected to increase with ion flux, but an increased ion flux can also cause elevated background signals, so the signal to noise ratio will not always improve with an increased reagent ion flux. In our hands, we have found that CTD reaction times in the range of 30-100 ms generally provide the best signal-to-noise ratios for product ion spectra, even though the CTD efficiencies are not necessarily maximized at these short reaction times. Methods to reduce the chemical background would enable higher reagent ion fluxes or longer reaction times, both of which would enhance the signal to noise ratios of CTD spectra.

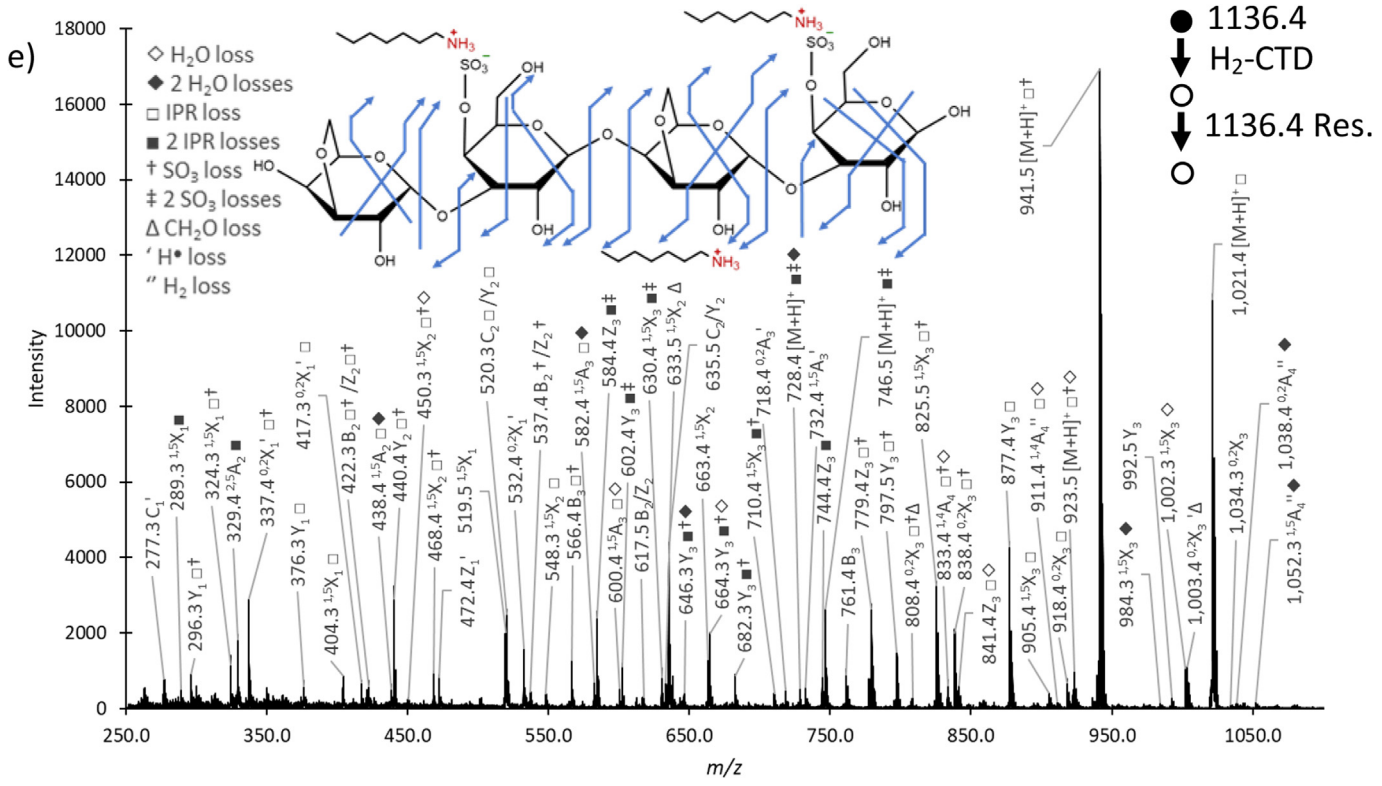

Fig. 6. (*continued*).

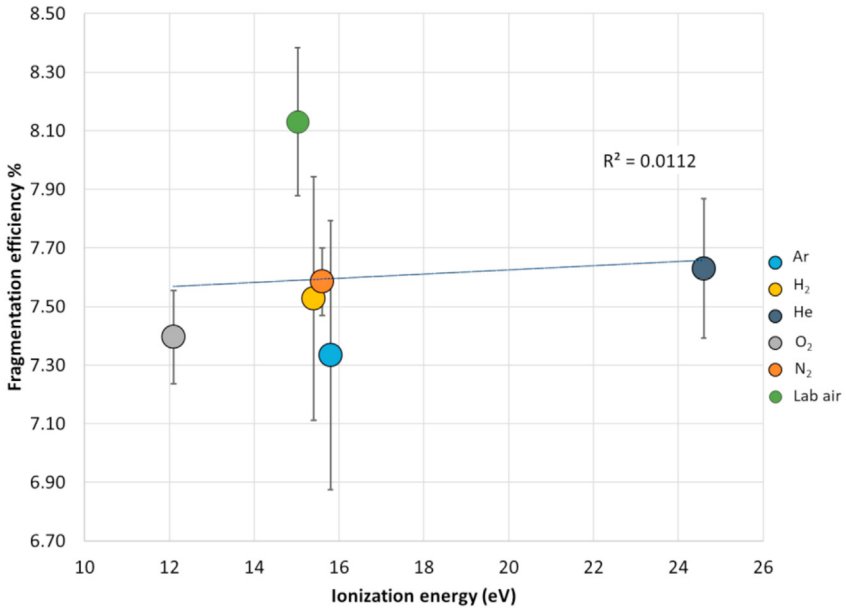

Fig. 7. CTD reagent gas fragmentation efficiencies for κ-carrageenan dp4. Error bars show the 95% confidence interval for N=5 replicate experiments.

4. Conclusions

This work explored a variety of reagent gases for CTD-MS to determine if a more cost-effective and readily accessible substitute to helium could be found for the analysis of peptides and oligosaccharides. The two metrics of concern were the fragmentation efficiency and the level of structural information made available by the distribution of product ions. A direct comparison between reagent gases was performed by keeping constant the precursor ion abundance, the reagent ion kinetic energy and the reagent ion flux for two well-characterized biological molecules. The reagent gases studied included H_2, He, N_2, O_2, lab air and Ar. For bradykinin 1+, there were minimal differences in the types and relative abundances of product ions formed between the six different reagent gases, so the sequence coverage was quite independent of the reagent gas. The six studied reagent gases for CTD outperformed LE-CID for sequence coverage. Regarding efficiencies of fragmentation, LE-CID was considerably more efficient than all the CTD spectra, and fragmentation efficiencies for CTD ranged from 11-13%. Within this tight range, the CTnoD peak abundance and the CTD efficiency for bradykinin correlated strongly with the ionization energy of the reagent gas. However, the shallow slopes indicate that resonant charge transfer from the peptide ion's highest occupied molecular orbital (HOMO) to the reagent cation's lowest unoccupied orbital is a minor contributor to the overall population of activated peptide ions. Instead, the majority of the peptide ions are activated by the electron stopping mechanism, wherein electron excitation in the peptide ion is induced by long range coupling of electron−hole pairs.

The analysis of κ-carrageenan dp4 1+ did not reveal any practical differences in the abundance or types of ions generated with the six different reagent gases, and each reagent gas localized the sulfate groups with similar accuracy. The CTD efficiencies for all six gases was in the range of 7.3-8.1%. Although LE-CID was an order of magnitude more efficient than CTD, very little structural information could be gleaned from the LE-CID spectrum of κ-carrageenan dp4. Unlike bradykinin, the CTD fragmentation efficiencies of the highly sulfated κ-carrageenan dp4 do not correlate with the ionization energy of the reagent gas, so resonant charge transfer contributes less to the activation of this larger, electron-rich target ion than for bradykinin. Assuming these two model compounds are reasonably representative of their biological classes, structural characterization of peptides and oligosaccharides by CTD-MS can be performed with any of the six tested reagent gases, including nitrogen and lab air, without sacrificing the sequence coverage or fragmentation efficiency. None of the reagent gases showed any evidence of covalent bonding between the reagent gases and any of the product ions. Generally speaking, lab air, nitrogen, oxygen and hydrogen are less expensive than helium and argon, so these gases have an obvious advantage. If one chooses to use lab air or oxygen as reagent gases, care should be taken to ensure that the potential reactivity of these gases do not deleteriously impact the chemical background signal or sensitive components in the vacuum chamber. Because of its flammability, gas lines should be inspected to ensure that there are no leaks when using hydrogen.

Declaration of competing interest

The authors declare that they have no known competing financial interests or personal relationships that could have appeared to influence the work reported in this paper.

Acknowledgements

We thank Dr. David Ropartz and Dr. Hélène Rogniaux for helpful discussions and for supplying the carrageenan standard. The authors acknowledge financial support from the National Science Foundation (NSF) CHE-1710376 and the National Institute of Health (NIH) 1R01GM114494-01. The opinions, findings, and conclusions or recommendations expressed in this publication are those of the authors and do not necessarily reflect the views of the NSF or NIH.

Appendix A. Supplementary data

Supplementary data to this article can be found online at https://doi.org/10.1016/j.ijms.2021.116532.

References

[1] F. Meier, P.E. Geyer, S. Virreira Winter, J. Cox, M. Mann, BoxCar acquisition method enables single-shot proteomics at a depth of 10,000 proteins in 100 minutes, Nat. Methods 15 (2018) 440–448, https://doi.org/10.1038/s41592-018-0003-5.

[2] A. Makarov, Electrostatic axially harmonic orbital trapping: a high-performance technique of mass analysis, Anal. Chem. 72 (6) (2000) 1156–1162, https://doi.org/10.1021/ac991131p.

[3] Q. Hu, R.J. Noll, H. Li, A. Makarov, M. Hardman, R. Graham Cooks, The Orbitrap: a new mass spectrometer, J. Mass Spectrom. 40 (4) (2005) 430–443, https://doi.org/10.1002/jms.856.

[4] R.A. Zubarev, A. Makarov, Orbitrap mass spectrometry, Anal. Chem. 85 (11) (2013) 5288–5296, https://doi.org/10.1021/ac4001223.

[5] A.K. Shukla, J.H. Futrell, Tandem mass spectrometry: dissociation of ions by collisional activation, J. Mass Spectrom. 35 (2000) 1069–1090.

[6] S.A. McLuckey, Principles of collisional activation in analytical mass spectrometry, J. Am. Soc. Mass Spectrom. 3 (1992) 599–614.

[7] S.A. McLuckey, G.J.V. Berkel, D.E. Goeringer, G.L. Glish, Ion trap mass spectrometry of externally generated ions, Anal. Chem. 66 (13) (1994) 689–696, https://doi.org/10.1021/ac00085a001.

[8] P. Bayat, D. Lesage, R.B. Cole, Tutorial: ion activation in tandem mass spectrometry using ultra-high resolution instrumentation, Mass Spectrom. Rev. 39 (5–6) (2020) 680–702, https://doi.org/10.1002/mas.21623.

[9] S.A. McLuckey, D.E. Goeringer, Slow heating methods in tandem mass spectrometry, J. Mass Spectrom. 32 (1997) 461–474.

[10] M.S. Blevins, D.R. Klein, J.S. Brodbelt, Localization of cyclopropane modifications in bacterial lipids via 213 nm ultraviolet photodissociation mass spectrometry, Anal. Chem. 91 (10) (2019) 6820–6828, https://doi.org/10.1021/acs.analchem.9b01038.

[11] P. Yang, F. Xu, H.F. Li, Y. Wang, F.C. Li, M.Y. Shang, G.X. Liu, X. Wang, S.Q. Cai, Detection of 191 taxifolin metabolites and their distribution in rats using HPLC-ESI-IT-TOF-MS(n), Molecules 21 (9) (2016) 1–26, https://doi.org/10.3390/molecules21091209.

[12] L. Sleno, D.A. Volmer, Ion activation methods for tandem mass spectrometry, J. Mass Spectrom. 39 (10) (2004) 1091–1112, https://doi.org/10.1002/jms.703.

[13] J. Mitchell Wells, S.A. McLuckey, Collision-induced dissociation (CID) of peptides and proteins, in: A.L. Burlingame (Ed.), Methods in Enzymology, vol. 402, Academic Press, 2005, pp. 148–185.

[14] B. Paizs, S. Suhai, Fragmentation pathways of protonated peptides, Mass Spectrom. Rev. 24 (4) (2005) 508–548, https://doi.org/10.1002/mas.20024.

[15] R.E. March, An introduction to quadrupole ion trap mass spectrometry, J. Mass Spectrom. 32 (1997) 351–369.

[16] R.E. March, J.F.J. Todd, Quadrupole Ion Trap Mass Spectrometry, second ed., vol. 165, John Wiley & Sons, Inc., Hoboken, New Jersey, 2005.

[17] J.N. Louris, R.G. Cooks, J.E.P. Syka, P.E. Kelley, G.C. Stafford Jr., J.F.J. Todd, Instrumentation, applications, and energy deposition in quadrupole ion-trap tandem mass spectrometry, Anal. Chem. 59 (13) (1987) 1677–1685, https://doi.org/10.1021/ac00140a021.

[18] B.M. Prentice, R.E. Santini, S.A. McLuckey, Adaptation of a 3-D quadrupole ion trap for dipolar DC collisional activation, J. Am. Soc. Mass Spectrom. 22 (9) (2011) 1486–1492, https://doi.org/10.1007/s13361-011-0183-z.

[19] B.M. Prentice, W. Xu, Z. Ouyang, S.A. McLuckey, DC potentials applied to an end-cap electrode of a 3-D ion trap for enhanced MS functionality, Int. J. Mass Spectrom. 306 (2–3) (2011) 114–122, https://doi.org/10.1016/j.ijms.2010.09.022.

[20] G.P. Jackson, J.J. Hyland, Ü.A. Laskay, Energetics and efficiencies of collision-induced dissociation achieved during the mass acquisition scan in a quadrupole ion trap, Rapid Commun. Mass Spectrom. 19 (23) (2005) 3555–3563, https://doi.org/10.1002/rcm.2228.

[21] O.L. Collin, M. Beier, G.P. Jackson, Dynamic collision-induced dissociation of peptides in a quadrupole ion trap mass spectrometer, Anal. Chem. 79 (14) (2007) 5468–5473, https://doi.org/10.1021/ac0707683.

[22] U.A. Laskay, J.J. Hyland, G.P. Jackson, Dynamic collision-induced dissociation (DCID) in a quadrupole ion trap using a two-frequency excitation waveform: I. Effects of excitation frequency and phase angle, J. Am. Soc. Mass Spectrom. 18 (4) (2007) 749–761, https://doi.org/10.1016/j.jasms.2006.12.008.

[23] U.A. Laskay, O.L. Collin, J.J. Hyland, B. Nichol, G.P. Jackson, S.P. Pasilis, D.C. Duckworth, Dynamic collision-induced dissociation (DCID) in a quadrupole ion trap using a two-frequency excitation waveform: II. Effects of frequency spacing and scan rate, J. Am. Soc. Mass Spectrom. 18 (11) (2007) 2017–2025, https://doi.org/10.1016/j.jasms.2007.08.014.

[24] C. Cunningham Jr., G.L. Glish, D.J. Burinsky, High amplitude short time excitation: a method to form and detect low mass product ions in a quadrupole ion trap mass spectrometer, J. Am. Soc. Mass Spectrom. 17 (1) (2006) 81–84, https://doi.org/10.1016/j.jasms.2005.09.007.

[25] J.C. Schwartz, High-Q pulsed fragmentation in ion traps, U.S. Patent US20070295903A1, December 27 (2007).

[26] R.A. Zubarev, N.L. Kelleher, F.W. McLafferty, Electron capture dissociation of multiply charged protein cations, A Nonergodic Process. J. Am. Chem. Soc. 120 (1998) 3265–3266.

[27] B.A. Budnik, K.F. Haselmann, R.A. Zubarev, Electron detachment dissociation of peptide di-anions: an electron-hole recombination phenomenon, Chem. Phys. Lett. 342 (2001) 299–302.

[28] S.L. Cook, O.L. Collin, G.P. Jackson, Metastable atom-activated dissociation mass spectrometry: leucine/isoleucine differentiation and ring cleavage of proline residues, J. Mass Spectrom. 44 (8) (2009) 1211–1223, https://doi.org/10.1002/jms.1598.

[29] V.D. Berkout, Fragmentation of protonated peptide ions via interaction with metastable Atoms, Anal. Chem. 78 (9) (2006) 3055–3061, https://doi.org/10.1021/ac060069a.

[30] V.D. Berkout, Fragmentation of singly protonated peptides via interaction with metastable rare gas atoms, Anal. Chem. 81 (2) (2009) 725–731, https://doi.org/10.1021/ac802214e.

[31] A.S. Misharin, O.A. Silivra, F. Kjeldsen, R.A. Zubarev, Dissociation of peptide ions by fast atom bombardment in a quadrupole ion trap, Rapid Commun. Mass Spectrom. 19 (15) (2005) 2163–2171, https://doi.org/10.1002/rcm.2038.

[32] K. Chingin, A. Makarov, E. Denisov, O. Rebrov, R.A. Zubarev, Fragmentation of positively-charged biological ions activated with a beam of high-energy cations, Anal. Chem. 86 (1) (2014) 372–379, https://doi.org/10.1021/ac403193k.

[33] S. Bari, R. Hoekstra, T. Schlathölter, Peptide fragmentation by keV ion-induced dissociation, Phys. Chem. Chem. Phys. 12 (14) (2010) 3376–3383, https://doi.org/10.1039/c004156b.

[34] S. Bari, R. Hoekstra, T. Schlathölter, Fast side-chain losses in keV ion-induced dissociation of protonated peptides, Int. J. Mass Spectrom. 299 (2010) 64–70, https://doi.org/10.1016/j.ijms.2010.09.019.

[35] J.E. Syka, J.J. Coon, M.J. Schroeder, J. Shabanowitz, D.F. Hunt, Peptide and protein sequence analysis by electron transfer dissociation mass spectrometry, Proc. Natl. Acad. Sci. U.S.A. 101 (26) (2004) 9528–9533, https://doi.org/10.1073/pnas.0402700101.

[36] J.J. Coon, J. Shabanowitz, D.F. Hunt, J.E. Syka, Electron transfer dissociation of peptide anions, J. Am. Soc. Mass Spectrom. 16 (6) (2005) 880–882, https://doi.org/10.1016/j.jasms.2005.01.015.

[37] T. Ly, R.R. Julian, Ultraviolet photodissociation: developments towards applications for mass-spectrometry-based proteomics, Angew. Chem. Int. Ed. 48 (39) (2009) 7130–7137, https://doi.org/10.1002/anie.200900613.

[38] J.S. Brodbelt, J.J. Wilson, Infrared multiphoton dissociation in quadrupole ion traps, Mass Spectrom. Rev. 28 (3) (2009) 390–424, https://doi.org/10.1002/mas.20216.

[39] J.P. Reilly, Ultraviolet photofragmentation of biomolecular ions, Mass Spectrom. Rev. 28 (3) (2009) 425–447, https://doi.org/10.1002/mas.20214.

[40] J.W. Morgan, J.M. Hettick, D.H. Russell, Peptide sequencing by MALDI 193-nm photodissociation TOF MS, in: A.L. Burlingame (Ed.), Methods in Enzymology, vol. 402, Academic Press, 2005, pp. 186–209.

[41] V.H. Wysocki, J.-M. Ding, J.L. Jones, J.H. Callahan, F.L. King, Surface-induced dissociation in tandem quadrupole mass spectrometers: a comparison of three designs, J. Am. Soc. Mass Spectrom. 3 (1992) 27–32.

[42] MdA. Mabud, M.J. Dekrey, R.G. Cooks, Surfaced-induced dissociation of molecular ions, Int. J. Mass Spectrom. Ion Process. 67 (1985) 285–294.

[43] D.T. Snyder, E. Panczyk, A.Q. Stiving, J.D. Gilbert, A. Somogyi, D. Kaplan, V. Wysocki, Design and performance of a second-generation surface-induced dissociation cell for fourier transform ion cyclotron resonance mass spectrometry of native protein complexes, Anal. Chem. 91 (21) (2019) 14049–14057, https://doi.org/10.1021/acs.analchem.9b03746.

[44] W.D. Hoffmann, G.P. Jackson, Charge transfer dissociation (CTD) mass spectrometry of peptide cations using kiloelectronvolt HeliumCations, J. Am. Soc. Mass Spectrom. 25 (11) (2014) 1939–1943, https://doi.org/10.1007/s13361-014-0989-6.

[45] G.P. Jackson, W.D. Hoffmann, Method and Device for Mass Spectrometric Analysis of Biomolecules Using Charge Transfer Dissociation, US9997342B2, 2018.

[46] D. Ropartz, P. Li, M. Fanuel, A. Giuliani, H. Rogniaux, G.P. Jackson, Charge transfer dissociation of complex oligosaccharides: comparison with collision-induced dissociation and extreme ultraviolet dissociative photoionization, J. Am. Soc. Mass Spectrom. 27 (10) (2016) 1614–1619, https://doi.org/10.1007/s13361-016-1453-6.

[47] D. Ropartz, A. Giuliani, M. Fanuel, C. Herve, M. Czjzek, H. Rogniaux, Online coupling of high-resolution chromatography with extreme UV photon activation tandem mass spectrometry: application to the structural investigation of complex glycans by dissociative photoionization, Anal. Chim. Acta 933 (2016) 1–9, https://doi.org/10.1016/j.aca.2016.05.036.

[48] P. Li, G.P. Jackson, Charge transfer dissociation (CTD) mass spectrometry of peptide cations: study of charge state effects and side-chain losses, J. Am. Soc. Mass Spectrom. 28 (7) (2017) 1271–1281, https://doi.org/10.1007/s13361-016-1574-y.

[49] D. Ropartz, P. Li, G.P. Jackson, H. Rogniaux, Negative polarity helium charge transfer dissociation tandem mass spectrometry: radical-initiated fragmentation of complex polysulfated anions, Anal. Chem. 89 (7) (2017) 3824–3828, https://doi.org/10.1021/acs.analchem.7b00473.

[50] L.E. Pepi, Z.J. Sasiene, P.M. Mendis, G.P. Jackson, I.J. Amster, Structural characterization of sulfated glycosaminoglycans using charge-transfer dissociation, J. Am. Soc. Mass Spectrom. 31 (10) (2020) 2143–2153, https://doi.org/10.1021/jasms.0c00252.

[51] P. Li, I. Kreft, G.P. Jackson, Top-down charge transfer dissociation (CTD) of gas-phase insulin: evidence of a one-step, two-electron oxidation mechanism, J. Am. Soc. Mass Spectrom. 29 (2) (2018) 284–296, https://doi.org/10.1007/s13361-017-1700-5.

[52] P. Li, G.P. Jackson, Charge transfer dissociation of phosphocholines: gas-phase

ion/ion reactions between helium cations and phospholipid cations, J. Mass Spectrom. 52 (5) (2017) 271–282, https://doi.org/10.1002/jms.3926.
[53] H. Buck-Wiese, M. Fanuel, M. Liebeke, K. Le Mai Hoang, A. Pardo-Vargas, P.H. Seeberger, J.H. Hehemann, H. Rogniaux, G.P. Jackson, D. Ropartz, Discrimination of beta-1,4- and beta-1,3-linkages in native oligosaccharides via charge transfer dissociation mass spectrometry, J. Am. Soc. Mass Spectrom. 31 (6) (2020) 1249–1259, https://doi.org/10.1021/jasms.0c00087.
[54] A. Cho, Helium-3 shortage could put freeze on low-temperature research, Science 326 (2009) 778–779, https://doi.org/10.1126/science.326_778.
[55] W.J. Nuttall, R.H. Clarke, B.A. Glowacki, Stop squandering helium, Nature 485 (2012) 573–575.
[56] W.P. Halperin, The impact of helium shortages on basic research, Nat. Phys. 10 (7) (2014) 467–470, https://doi.org/10.1038/nphys3018.
[57] A.J. Hurd, R.L. Kelley, R.G. Eggert, M.-H. Lee, Energy-critical elements for sustainable development, MRS Bull. 37 (4) (2012) 405–410, https://doi.org/10.1557/mrs.2012.54.
[58] S.M. Fortier, N.T. Nassar, G.W. Lederer, J. Brainard, J. Gambogi, E.A. McCullough, U.S. Department of the interior: draft critical mineral list—summary of methodology and background information—U.S. Geological survey technical input document in response to secretarial order 3359 (2018) 1–15, https://doi.org/10.3133/ofr20181021.
[59] D.A. Shea, D. Morgan, in: C.R. Service (Ed.), The Helium-3 Shortage: Supply, Demand, and Options for Congress, 2010, pp. 1–27.
[60] V.D. Berkout, V.M. Doroshenko, Fragmentation of phosphorylated and singly charged peptide ions via interaction with metastable atoms, Int. J. Mass Spectrom. 278 (2–3) (2008) 150–157, https://doi.org/10.1016/j.ijms.2008.04.019.
[61] K.M. Downard, K. Biemann, The effect of charge state and the localization of charge on the collision-induced dissociation of peptide ions, J. Am. Soc. Mass Spectrom. 5 (1994) 966–975.
[62] S.A. Robotham, J.S. Brodbelt, Comparison of ultraviolet photodissociation and collision induced dissociation of adrenocorticotropic hormone peptides, J. Am. Soc. Mass Spectrom. 26 (9) (2015) 1570–1579, https://doi.org/10.1007/s13361-015-1186-y.
[63] J.W. Morgan, D.H. Russell, Comparative studies of 193-nm photodissociation and TOF-TOFMS analysis of bradykinin analogues: the effects of charge site(s) and fragmentation timescales, J. Am. Soc. Mass Spectrom. 17 (5) (2006) 721–729, https://doi.org/10.1016/j.jasms.2006.02.004.
[64] Y.M.E. Fung, C.M. Adams, R.A. Zubarev, Electron ionization dissociation of singly and multiply charged peptides, J. Am. Chem. Soc. 131 (29) (2009) 9977–9985, https://doi.org/10.1021/ja8087407.
[65] F. Canon, A.R. Milosavljevic, L. Nahon, A. Giuliani, Action spectroscopy of a protonated peptide in the ultraviolet range, Phys. Chem. Chem. Phys. 17 (39) (2015) 25725–25733, https://doi.org/10.1039/c4cp04762a.
[66] Y.M. Fung, T.W. Chan, Experimental and theoretical investigations of the loss of amino acid side chains in electron capture dissociation of model peptides, J. Am. Soc. Mass Spectrom. 16 (9) (2005) 1523–1535, https://doi.org/10.1016/j.jasms.2005.05.001.
[67] S.B. Nielsen, J.U. Andersen, P. Hvelplund, T.J.D. Jørgensen, M. Sørensena, S. Tomitaa, Triply charged bradykinin and gramicidin radical cations: their formation and the selective enhancement of charge-directed cleavage processes, Int. J. Mass Spectrom. 213 (2002) 225–235.
[68] K. Biemann, Sequencing of peptides by tandem mass spectrometry and high-energy collision-induced dissociation, in: J.A. McCloskey (Ed.), Methods in Enzymology, vol. 193, 1990, pp. 455–479.
[69] L. Poulter, L.C.E. Taylor, A comparison of low and high energy collisionally activated decompostion MS-MS for peptide sequencing, Int. J. Mass Spectrom. Ion Process. 91 (2) (1989) 183–197, https://doi.org/10.1016/0168-1176(89)83008-3.
[70] J. Laskin, Z. Yang, C.M. Ng, I.K. Chu, Fragmentation of alpha-radical cations of arginine-containing peptides, J. Am. Soc. Mass Spectrom. 21 (4) (2010) 511–521, https://doi.org/10.1016/j.jasms.2009.12.021.
[71] H.J. Cooper, R.R. Hudgins, Kristina Håkansson, A.G. Marshall, Characterization of amino acid side chain losses in electron capture dissociation, J. Am. Soc. Mass Spectrom. 13 (2002) 241–249.
[72] K.M. Zia, S. Tabasum, M. Nasif, N. Sultan, N. Aslam, A. Noreen, M. Zuber, A review on synthesis, properties and applications of natural polymer based carrageenan blends and composites, Int. J. Biol. Macromol. 96 (2017) 282–301, https://doi.org/10.1016/j.ijbiomac.2016.11.095.
[73] J. Necas, L. Bartosikova, Carrageenan: a review, Vet. Med. Czech 58 (4) (2013) 187–205, https://doi.org/10.17221/6758-VETMED.
[74] T. Wyttenbach, G.v. Helden, M.T. Bowers, Gas-phase conformation of biological molecules: bradykinin, J. Am. Chem. Soc. 118 (35) (1996) 8355–8364, https://doi.org/10.1021/ja9535928.